


Article

Optimization of Extraction Conditions from Gac Fruit and Utilization of Peel-Derived Biochar for Crystal Violet Dye Removal

Nhat-Thien Nguyen¹, Pin-Ru Chen¹, Ru-Hau Ye¹, Kai-Jen Chuang^{2,3} , Chang-Tang Chang^{4,*} and Gui-Bing Hong^{1,*}

¹ Department of Chemical Engineering and Biotechnology, National Taipei University of Technology, No. 1, Sec. 3, Zhongxiao E. Rd., Taipei 106, Taiwan; nguyennhatthien333@gmail.com (N.-T.N.); slulu8673@gmail.com (P.-R.C.); k050614@gmail.com (R.-H.Y.)

² School of Public Health, College of Public Health and Nutrition, Taipei Medical University, Taipei 110, Taiwan; kjc@tmu.edu.tw

³ Department of Public Health, School of Medicine, College of Medicine, Taipei Medical University, Taipei 110, Taiwan

⁴ Department of Environmental Engineering, National Ilan University, Yilan City 260, Taiwan

* Correspondence: ctchang@niu.edu.tw (C.-T.C.); lukehong@ntut.edu.tw (G.-B.H.); Tel.: +886-2-2771-2171 (G.-B.H.)

Abstract: Gac fruit (*Momordica cochinchinensis* Spreng.) is a prominent source of carotenoids, renowned for its exceptional concentration of these compounds. This study focuses on optimizing the extraction of active components from the aril of gac fruit by evaluating the effects of extraction temperature, solid–liquid ratio, and extraction time. The primary objective is to maximize the yield of gac oil while assessing its antioxidant capacity. To analyze the kinetics of the solid–liquid extraction process, both first-order and second-order kinetic models were employed, with the second-order model providing the best fit for the experimental data. In addition, the potential of gac fruit peel as a precursor for biochar production was investigated through carbonization. The resultant biochars were evaluated for their efficacy in adsorbing crystal violet (CV) dye from aqueous solutions. The adsorption efficiency of the biochars was found to be dependent on the carbonization temperature, with the highest efficiency observed for BCMC550 (91.72%), followed by BCM450 (81.35%), BCMC350 (78.35%), and BCMC250 (54.43%). The adsorption isotherm data conformed well to the Langmuir isotherm model, indicating monolayer adsorption behavior. Moreover, the adsorption kinetics were best described by the pseudo-second-order model. These findings underscore the potential of gac fruit and its byproducts for diverse industrial and environmental applications, highlighting the dual benefits of optimizing gac oil extraction and utilizing the peel for effective dye removal.

Keywords: extraction; *Momordica cochinchinensis* Spreng.; adsorbent; crystal violet



Citation: Nguyen, N.-T.; Chen, P.-R.; Ye, R.-H.; Chuang, K.-J.; Chang, C.-T.; Hong, G.-B. Optimization of Extraction Conditions from Gac Fruit and Utilization of Peel-Derived Biochar for Crystal Violet Dye Removal. *Molecules* **2024**, *29*, 3435. <https://doi.org/10.3390/molecules29143435>

Academic Editor: Dimitrios Kalderis

Received: 21 June 2024

Revised: 19 July 2024

Accepted: 19 July 2024

Published: 22 July 2024



Copyright: © 2024 by the authors. Licensee MDPI, Basel, Switzerland. This article is an open access article distributed under the terms and conditions of the Creative Commons Attribution (CC BY) license (<https://creativecommons.org/licenses/by/4.0/>).

1. Introduction

Momordica cochinchinensis Spreng., commonly referred to as gac fruit, is a perennial plant of the genus *Momordica* within the Cucurbitaceae family. This botanical species was initially documented as *Muricia cochinchinensis* by the Portuguese missionary Loureiro during his exploration of Vietnam in 1790. Subsequently, Sprengel reassigned the species to the Linnaean genus *Momordica*, leading to the alteration of its scientific nomenclature in 1826 [1]. Indigenous to regions including Vietnam, Thailand, India, Southwest China, and Taiwan, gac fruit is distinguished by its exceptional lycopene content, exceeding that of tomatoes by over 70 times, and its abundance in carotenoids, vitamin E, and other essential constituents [2]. Afterwards, the cultivation of Southeast Asian varieties of gac fruit was introduced to Taiwan, where it was planted extensively in the central and southern regions. However, the native gac fruit from Taitung is renowned for its superior quality,

characterized by its sweet and mildly warm flavor, absence of oiliness, and lack of bitterness, setting it apart from its Southeast Asian counterparts. Comprising the exocarp, pulp, aril, seed, and connective tissue, gac fruit stands out as the fruit with the highest carotenoid content among all natural fruits and vegetables known to date. The aril of the gac fruit, particularly rich in lycopene and β -carotene, is esteemed for its nutrient density, earning it the monikers “super fruit” or “heaven’s fruit” [3].

Carotenoids are typically categorized into two groups: carotenes, which lack oxygen atoms and primarily include α -carotene, β -carotene, γ -carotene, and lycopene; and oxygen-containing carotenoids, such as lutein, zeaxanthin, and others. Due to their numerous physiological functions, including anti-inflammatory, antioxidant, cancer-preventive, vision maintenance, immune modulation, neuroprotective, and more, carotenoids have garnered significant attention from both domestic and international researchers, with a particular focus on lycopene and β -carotene [4]. There are various techniques available for extracting active ingredients, including distillation, cold pressure, solvent extraction [5], ultrasonic-assisted extraction [6], microwave-assisted extraction [7], and supercritical fluid extraction [8]. Among these, solvent extraction stands out as the most widely employed method for extracting vegetable oils and active compounds due to its simplicity, stability of extracts, high efficiency, and cost-effectiveness. Gac fruit is known for its high nutritional value and bioactive compounds, such as carotenoids and antioxidants [7]. Various extraction methods have been employed to maximize the yield and preserve the quality of these compounds. For instance, Wong et al. [6] reported on the efficiency of ultrasonic-assisted extraction for enhancing the extraction of carotenoids from gac fruit, demonstrating its potential for various applications.

Biochar derived from agricultural waste has garnered significant interest due to its potential for environmental remediation. Research has shown that biochar from various biomass sources can effectively remove contaminants from water, including dyes, heavy metals, and organic pollutants [9]. Crystal violet (CV) is a synthetic dye widely used in industries such as textiles, paper, and printing. It is known for its high stability and resistance to biodegradation, making it a persistent environmental pollutant. Numerous studies have demonstrated the efficacy of biochar in adsorbing dye molecules from aqueous solutions. CV dye, in particular, is frequently used as a model pollutant to evaluate the adsorption capacity of biochar. For example, Tran et al. [10] investigated the adsorption of CV using biochar derived from tea waste and observed significant removal efficiency, attributing it to the surface area and functional groups of the biochar. The removal of CV from wastewater is therefore of significant environmental concern [11]. Numerous studies have utilized CV dye as a model contaminant to evaluate the adsorption efficiency of various adsorbents. This facilitates the comparison of the adsorption performance of biochar from gac fruit peel with other adsorbents reported in the literature [12,13].

The extraction of antioxidant components from plants typically follows a solid–liquid extraction process. The determination of extraction kinetic parameters is crucial for designing an efficient extraction process [14,15]. Various solid–liquid extraction kinetic models are commonly used, including the Ponomaryov empirical formula [16], Peleg model [17], Fick diffusion law [18], and first-order kinetic models [19,20]. Despite numerous studies on antioxidant components extracted from natural plants, there is a notable dearth of data assessing the extraction kinetic models used for this purpose [21]. Therefore, this study focused on extracting arils from native gac fruit in Taitung and repurposing the residual peel of gac fruit, which is often discarded as waste, to create a value-added product—biochar. Due to their cost-effectiveness, ample availability, and potential for recycling, there is a viable opportunity to convert agricultural waste and by-products into adsorbent materials with enhanced value. The solid–liquid extraction process and the performance of biochar in CV adsorption will be evaluated using mathematical models.

2. Results and Discussion

2.1. Extraction Results

2.1.1. Effect of Extraction Temperature

In accordance with the findings of Lan et al. [22], lycopene and β -carotene exhibit notable absorption peaks in the UV/vis spectrum within the 400–500 nm range. These peaks are consistent with the characteristic absorption peaks of lycopene and, specifically, with those of β -carotene at 452 nm and 478 nm. As depicted in Figure 1a, at a solid–liquid ratio (S/L ratio) of 1/9 and an extraction duration of 30 min, the absorption intensity of the extract obtained at temperatures below 50 °C approached a similar level. However, the peak around 450 nm exhibited a significant increase as the temperature surpassed 50 °C, indicating an increase in lycopene content in the extract during the extraction process. As the temperature rose from 50 °C to 60 °C, carotenoid recovery increased rapidly, facilitated by the faster and easier removal of fatty acids from the cell wall and particles, leading to higher carotenoid concentrations. Correspondingly, the extraction yield, as well as the DPPH and ABTS radical scavenging abilities, exhibited an increase with the elevation of extraction temperature, as illustrated in Figure 1b–d. Elevating the extraction temperature can disrupt the phenolic-matrix bond and impact the membrane structure of plant cells, thereby enhancing the extraction efficiency of phenolic compounds. Nevertheless, excessively high extraction temperatures during heating may lead to the degradation of phenolic compounds, resulting in greater losses of components [23]. Consequently, subsequent extraction experiments were conducted at a constant temperature of 70 °C.

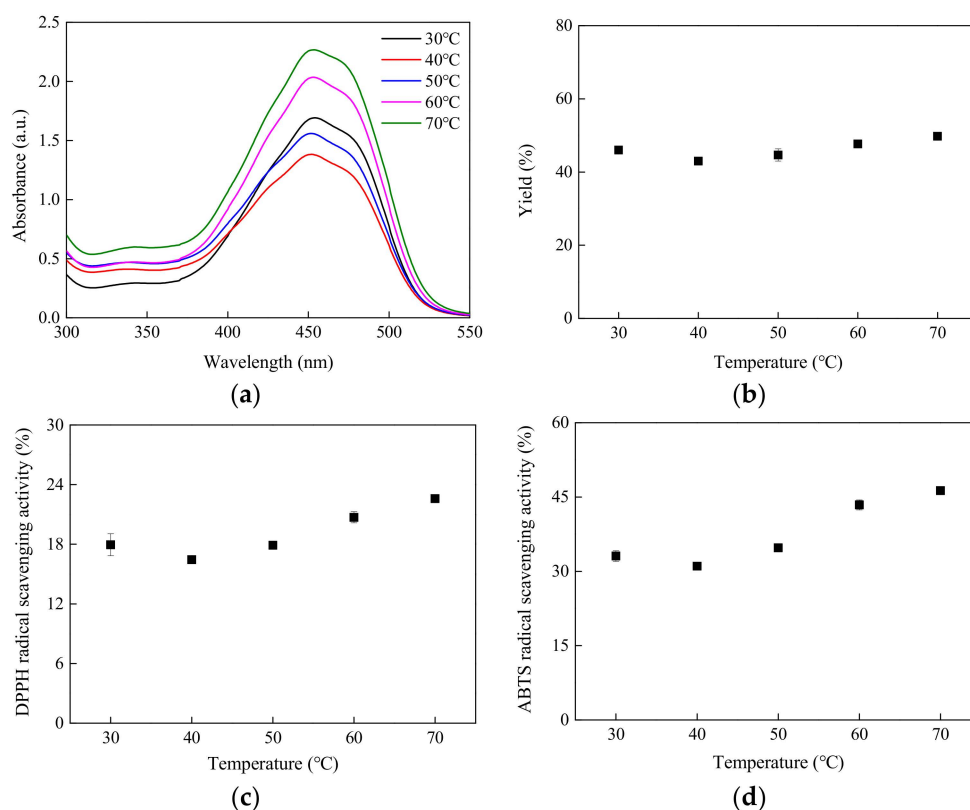


Figure 1. Temperature effect on (a) UV/vis spectrum, (b) extraction yield, (c) DPPH free radical scavenging ability, and (d) ABTS free radical scavenging ability.

2.1.2. Effect of S/L Ratio

The S/L ratio exerts a notable influence on the extraction process. The solvent plays a crucial role in expanding the material being extracted, necessitating complete immersion of the material in a sufficient volume of solvent to enhance extraction efficiency. Under the experimental conditions of a 70 °C extraction temperature and a 30 min extraction duration,

the impact of different S/L ratios is illustrated in Figure 2. As depicted in Figure 2a, with the S/L ratio gradually increasing from 1/1 to 1/5 and 1/9, there is a significant rise in the absorbance intensity of the extracted material within the 400–500 nm range. However, the adsorption strength starts to decline upon further increase in solvent volume. Generally, a higher solvent volume increases the likelihood of penetrating plant cells, potentially leading to higher yields of active ingredients. Nonetheless, excessive solvent may reduce the extraction of active ingredients due to inadequate stirring [24]. Similarly, it is evident that the extraction yield, as well as the DPPH and ABTS free radical scavenging capacities, increase with rising solvent volume until an S/L ratio of 1/13, beyond which they begin to decline, as depicted in Figure 2b–d.

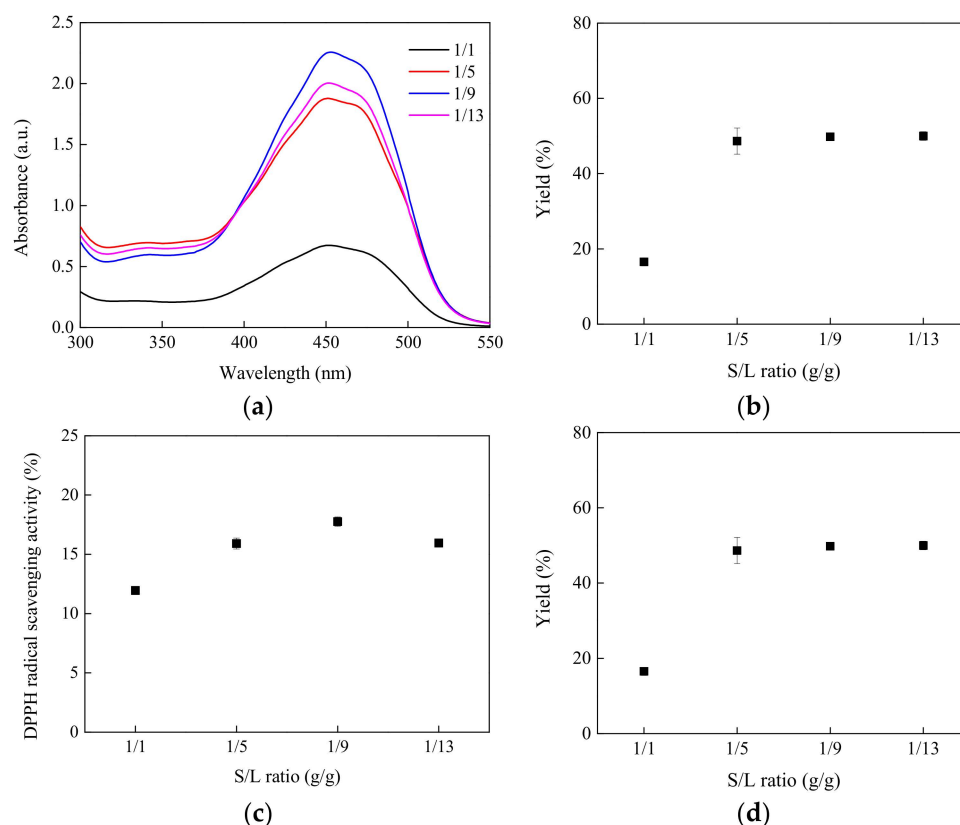


Figure 2. S/L ratio effect on (a) UV/vis spectrum, (b) extraction yield, (c) DPPH free radical scavenging ability, and (d) ABTS free radical scavenging ability.

2.1.3. Extraction Time Effect

The choice of extraction solvent polarity determines the substances that can be dissolved during the extraction process. In this experiment, ethanol, known for its lower toxicity, was utilized as the extraction solvent. Operating under conditions of 70 °C and an S/L ratio of 1/9, the impact of varying extraction times is illustrated in Figure 3. With an increase in extraction time, the absorption intensity (Figure 3a) of the extract in the UV/vis spectrum at 400–500 nm progressively rises, peaking at 120 min before declining. This trend is mirrored in the extraction yield, as well as the DPPH and ABTS radical scavenging capacities, as depicted in Figure 3b–d.

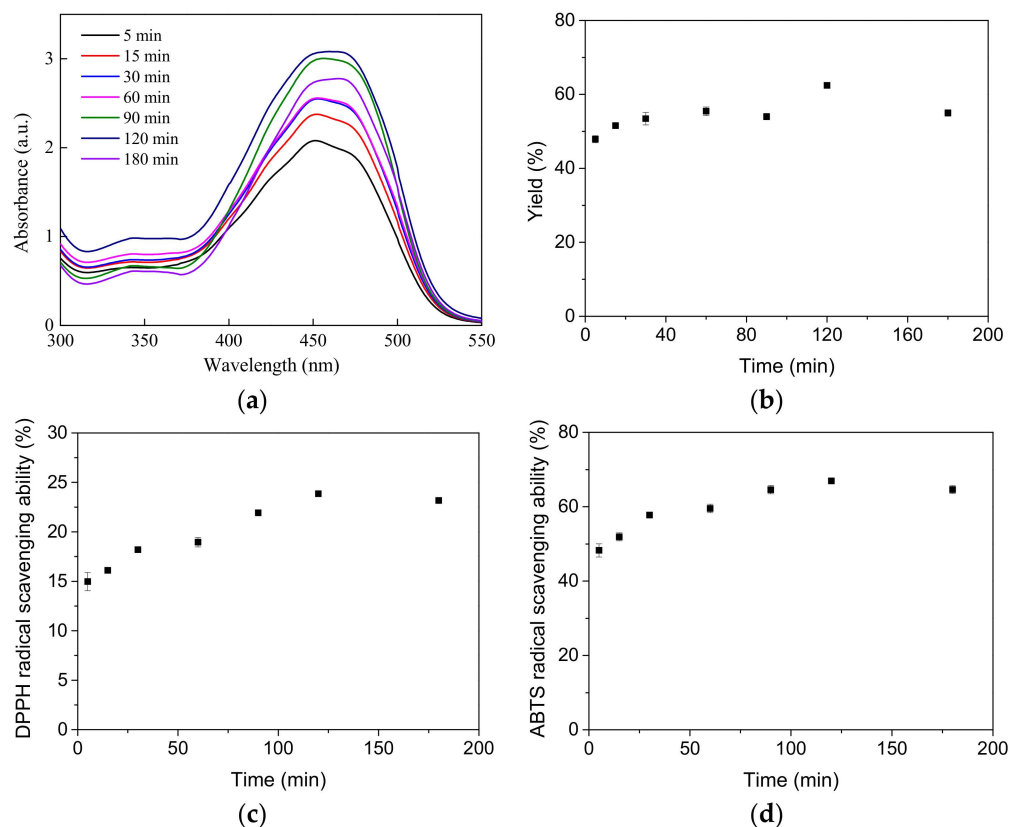


Figure 3. Extraction time effect on (a) UV/vis spectrum, (b) extraction yield, (c) DPPH free radical scavenging ability, (d) ABTS free radical scavenging ability.

2.1.4. Extraction Kinetics Data Calculation

Extraction kinetics experiments were conducted to elucidate the relationship between extraction yield and ascorbic acid (AA) equivalent over time, under conditions of an S/L ratio of 1/9 and a temperature of 70 °C. The experimental findings are presented in Figure 4. Both first-order and second-order kinetic models were employed to depict the extraction kinetics data. The results indicated that the second-order kinetic model provided a better fit ($R^2 > 0.98$) for both the extraction yield and ascorbic acid equivalent values compared to the first-order kinetic model. The parameters and model fitting results for each model are detailed in Table 1. Consequently, the extraction kinetics behavior of gac fruit can be suitably characterized using the second-order kinetic model.

Table 1. Calculation results of extraction kinetics models.

Models	Parameters	Yield	AA Equivalent
First-order kinetic model	k_1 (min^{-1})	0.019	0.038
	a	1.144	0.120
	R^2	0.406	0.813
Second-order kinetic model	k_2 ($\text{g} \cdot \text{g}^{-1} \text{min}^{-1}$)	2.610	0.004
	C_e	0.568	37.736
	R^2	0.994	0.981

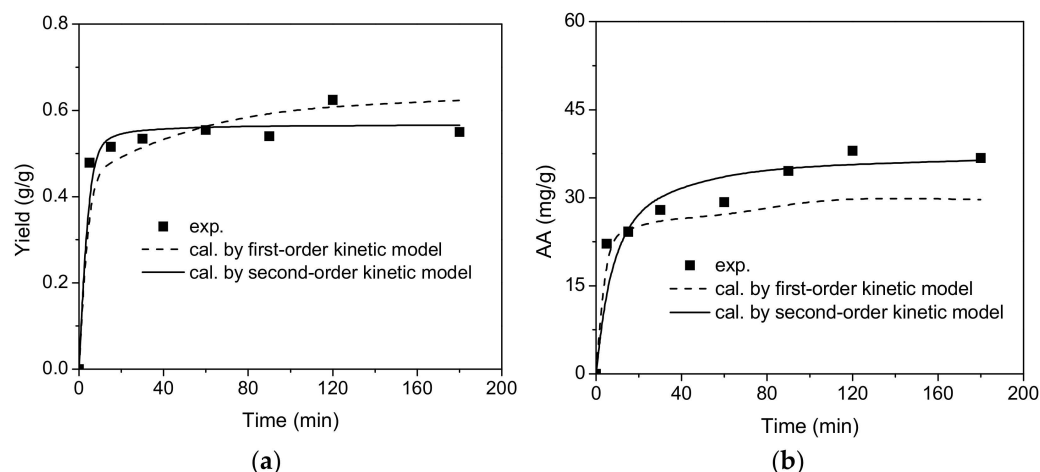


Figure 4. Extraction kinetics experimental results: (a) yield vs. time and (b) AA vs. time.

2.2. Characterization of Biochars

2.2.1. EA Result

To analyze the carbon proportions of gac fruit peel after carbonization at varying pyrolysis temperatures, an elemental analysis (EA) was utilized to determine the C, H, N, and S content of the biochars, as presented in Table 2. The carbon proportions of the biochars at different pyrolysis temperatures were 52.09%, 57.82%, 59.10%, and 62.98%, respectively, while the hydrogen (H) proportions were 4.769%, 2.898%, 2.030%, and 1.391%, respectively. The nitrogen (N) proportions were 1.95%, 1.86%, 1.66%, and 1.81%, respectively, and the sulfur (S) proportions were 0.00%, 1.324%, 0.637%, and 0.432%, respectively. The carbon content increased with rising pyrolysis temperature, reaching approximately 62.98% at 550 °C. Conversely, the proportions of H, N, and S decreased gradually with increasing pyrolysis temperature. The significant increase in C content, from 52.09% to 62.98%, suggests that most non-C elements in the gac fruit peel were volatilized during anaerobic roasting at pyrolysis temperatures ranging from 250 to 550 °C. The N proportion decreased by only 0.14%, from 1.95% to 1.81%, indicating that a substantial amount of N elements can be retained during low- to medium-temperature carbonization. Furthermore, the proportions of H decreased from 4.769% to 1.391%, while S decreased from 1.510% to 0.432%, showing limited variations.

Table 2. Elemental analysis results of biochars.

Biochars	N (%)	C (%)	H (%)	S (%)	C/N	C/H
BCMC250	1.95	52.09	4.769	1.510	26.73	10.92
BCMC350	1.86	57.82	2.898	1.324	31.05	19.95
BCMC450	1.66	59.10	2.030	0.637	35.63	29.12
BCMC550	1.81	62.98	1.391	0.432	34.77	45.28

2.2.2. SEM/EDS Analysis Result

To elucidate the surface morphology and elemental composition of carbonized gac fruit peel, an SEM/EDS analysis (Figure 5) was conducted. The EDS mapping results indicate a strong dominance of carbon on the biochar surface during pyrolysis. The combined SEM and EDS results reveal that pyrolysis produces a rougher oxygen surface with varied pores, which is favorable for the adsorption of CV dye. At a carbonization temperature of 250 °C, the biochar began to develop pores, although their number was not significant. As the temperature increased to 350 °C and beyond, the carbonization process exhibited improved efficacy, resulting in a greater number of evenly distributed pores. These findings indicate that the optimal carbonization condition was achieved at 550 °C.

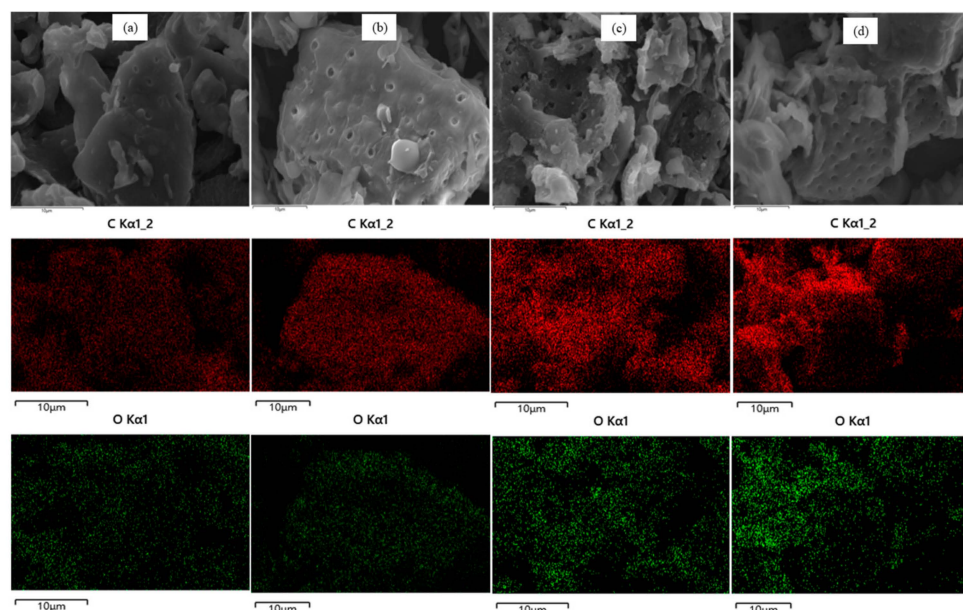


Figure 5. SEM/EDS analysis result of (a) BCMC250, (b) BCMC350, (c) BCMC450, and (d) BCMC550.

2.2.3. FTIR Analysis Results

Fourier-transform infrared spectroscopy (FTIR) was employed to analyze the functional groups present in the biochar derived from gac fruit peel. Figure 6 illustrates the variations in functional groups at different pyrolysis temperatures. The characteristic peaks of the CH_2 functional group, corresponding to the bending vibration of the C–H bond, were identified at 2930 cm^{-1} in the biochar [25]. The other peak at 1378 cm^{-1} shows the O–H bonding of phenolic functional group [26]. The peak intensity associated with the vibration of the phenolic group at approximately 3500 cm^{-1} exhibits a slight, albeit not significant, decrease with an increase in pyrolysis temperature. Furthermore, with increasing pyrolysis temperature, the intensity of certain functional groups diminishes or even disappears [27]. For instance, the bending vibration corresponding to the C = C bond near 1580 cm^{-1} [28] conspicuously decreases as the pyrolysis temperature rises. Upon comparing the FTIR spectra of BCMC550 before and after CV adsorption, the disappearance of bands at 3750 cm^{-1} (–NH), 2930 cm^{-1} (C–H), and 1010 cm^{-1} (N–O) confirms that CV effectively interacted with the functional groups on the biochar surface [27].

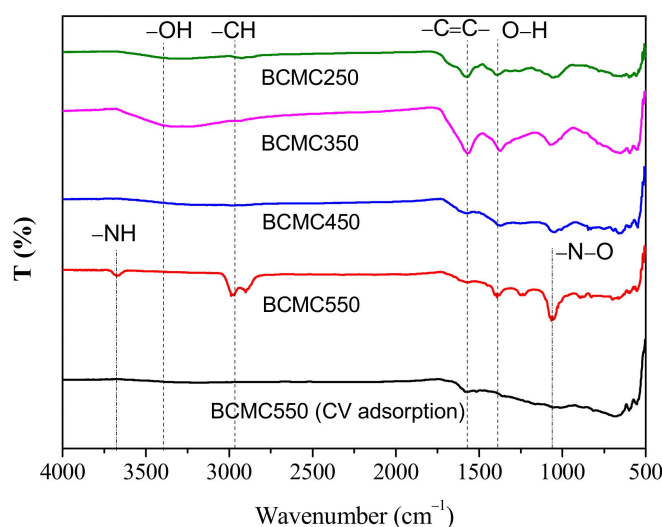


Figure 6. FTIR analysis of biochars.

2.2.4. BET Analysis Results

To investigate the surface area, pore size, and pore volume of biochars derived from gac fruit peel at various carbonization temperatures, nitrogen adsorption–desorption isotherms were employed. The specific surface area, pore size, and pore volume of the biochars were determined, and the results are summarized in Table 3. The specific surface areas of BCMC250, BCMC350, BCMC450, and BCMC550 were found to be 296, 313, 528, and 697 $\text{m}^2\cdot\text{g}^{-1}$, respectively. Correspondingly, the pore volumes were measured at 0.13, 0.18, 0.27, and 0.31 $\text{cm}^3\cdot\text{g}^{-1}$, respectively, with pore sizes of 2.05, 2.03, 2.07, and 2.03 nm, respectively. The biochars exhibited the highest specific surface area and pore volume for BCMC550, followed by BCMC450, with the smallest observed for BCMC250. This suggests that gac fruit peel undergoes optimal carbonization near 550 °C, as temperatures exceeding this may compromise the surface structure of the biochar, while temperatures lower than 450 °C may not produce a sufficient number of pores.

Table 3. BET analysis results of biochars.

Biochars	Surface Area ($\text{m}^2\cdot\text{g}^{-1}$)	Pore Volume ($\text{cm}^3\cdot\text{g}^{-1}$)	Pore Size (nm)
BCMC250	295.79	0.13	2.05
BCMC350	312.89	0.18	2.03
BCMC450	528.16	0.27	2.07
BCMC550	696.91	0.31	2.03

Figure 7 displays the nitrogen adsorption–desorption isotherms of biochar at different carbonization temperatures, illustrating that the N_2 adsorption/desorption isotherms of BCMC250, BCMC350, BCMC450, and BCMC550 conform to Type IV isotherms for mesoporous materials [29]. Overall, the biochar produced at 550 °C was found to be optimal, exhibiting a specific surface area of 697 $\text{m}^2\cdot\text{g}^{-1}$ and a pore volume of 0.31 $\text{cm}^3\cdot\text{g}^{-1}$.

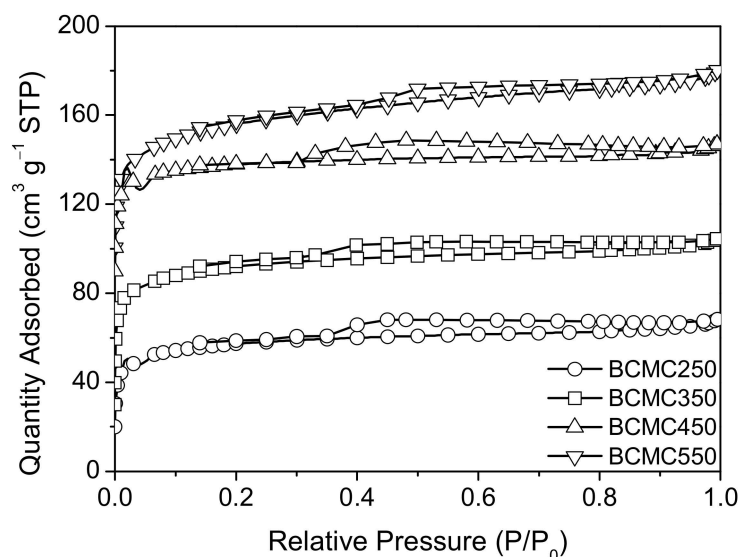


Figure 7. Nitrogen adsorption–desorption isotherms of biochars.

2.3. CV Adsorption Results

2.3.1. CV Dye Adsorption onto Different Biochars

To assess the adsorption capacity of biochar at different carbonization temperatures for CV dye, the adsorption performance of BCMC250, BCMC350, BCM450, and BCMC550 was compared. The adsorption experiments were conducted at 30 °C, with a CV dye concentration of 200 ppm, an adsorbent dose of 0.5 $\text{g}\cdot\text{L}^{-1}$, an adsorption time of 135 min, and a stirring speed of 100 rpm. A Shapiro–Wilk test was used to determine for

the normality of continuous variable. An analysis of variance (ANOVA) was utilized for between-group comparisons among different biochars, with a significance level of 0.05 and a two-sided distribution determining the statistical significance in our models. The results revealed that the CV removal efficiencies of BCMC250, BCMC350, BCMC450, and BCMC550 were 54.43%, 78.35%, 81.35%, and 91.72%, respectively, as illustrated in Figure 8 (p value < 0.05). The error bars in Figure 8 represent standard deviations. Among the biochars, BCMC550 exhibited the highest CV removal efficiency, attributed to the presence of functional groups on its surface that enhance CV dye adsorption, as indicated by the FTIR results (Figure 6). Furthermore, BCMC550 possessed the largest specific surface area ($697 \text{ m}^2 \cdot \text{g}^{-1}$), the highest pore volume ($0.31 \text{ cm}^3 \cdot \text{g}^{-1}$), and the highest carbon content (62.98%), all of which contribute to its superior adsorption performance.

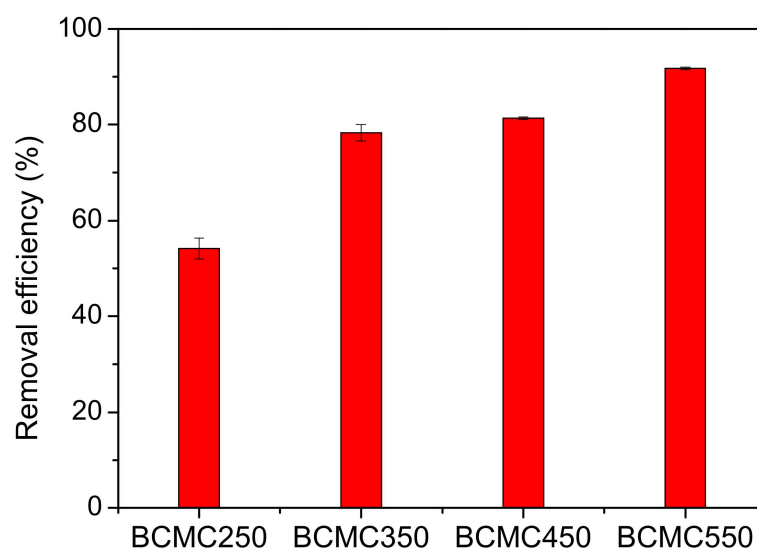


Figure 8. Adsorption results of CV dye onto biochars ($p < 0.05$).

2.3.2. Adsorption Kinetics Data of CV Dye Adsorption onto BCMC550

To investigate the adsorption capacity of BCMC550 biochar for CV dye following carbonization at $550 \text{ }^\circ\text{C}$, adsorption kinetic experiments were conducted under the following conditions: an adsorption temperature of $30 \text{ }^\circ\text{C}$, a CV concentration of 200 ppm, a BCMC550 dosage of $0.5 \text{ g} \cdot \text{L}^{-1}$, an adsorption time ranging from 0 to 480 min, and a stirring speed of 100 rpm. The adsorption kinetics data were analyzed by the pseudo-first-order [30] and pseudo-second-order [31] kinetic models to assess the most appropriate kinetic model. The correlated results, depicted in Figure 9a, b, revealed that the pseudo-second-order model exhibited a superior fit, with a correlation coefficient (R^2) value of 0.998, compared to the pseudo-first-order model, indicating its suitability for describing the adsorption of CV onto BCMC550. Table 4 provides a summary of the adsorption kinetics parameters derived from the adsorption kinetic models.

Table 4. Adsorption kinetic parameters for CV adsorption onto BCMC550.

Model	Parameters	
Pseudo-first-order	k_1 (min^{-1})	0.0149
	q_e ($\text{mg} \cdot \text{g}^{-1}$)	294.51
	R^2	0.974
Pseudo-second-order	k_2 ($\text{g} \cdot \text{mg}^{-1} \cdot \text{min}^{-1}$)	0.0001
	q_e ($\text{mg} \cdot \text{g}^{-1}$)	476.19
	R^2	0.998

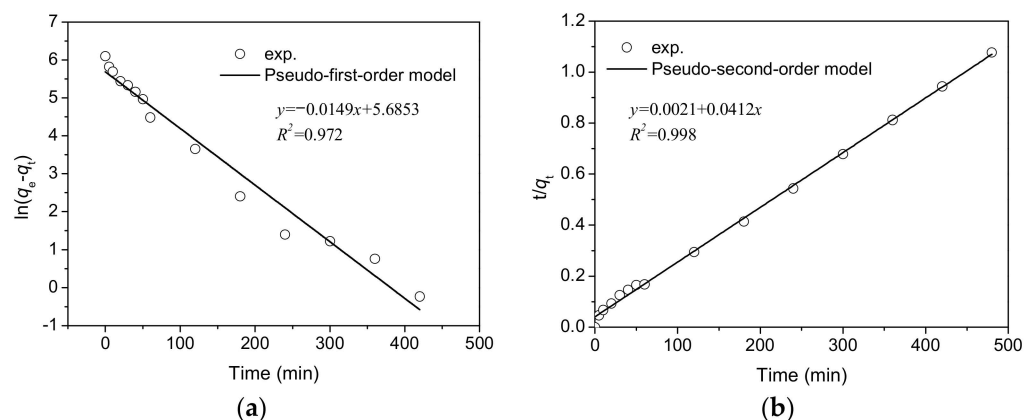


Figure 9. Correlation results of adsorption kinetics models: (a) pseudo-first-order; (b) pseudo-second-order.

2.3.3. Adsorption Isotherm Data of CV Dye Adsorption onto BCMC550

The adsorption isotherm data of CV adsorption onto BCMC550 were analyzed using the Langmuir [32] and Freundlich [33] adsorption isotherm models, as detailed in Table 5. The correlation results indicated that the Langmuir isotherm model exhibited a higher linear regression coefficient (R^2) compared to the Freundlich model, suggesting that the Langmuir model is more suitable for describing the isothermal adsorption behavior of CV onto BCMC550. The Langmuir adsorption isotherm model assumes monolayer coverage, negligible interactions between adsorbate molecules on adjacent sites, and uniform adsorption energy, thereby illustrating the adsorption behavior. This result suggests that CV dye is adsorbed onto the uniform surface of BCMC550, forming a monolayer with uniform adsorption energy. According to the Langmuir model, the maximum monolayer adsorption capacity (q_m) of BCMC550 biochar for CV is calculated to be $909.1 \text{ mg}\cdot\text{g}^{-1}$. Furthermore, the adsorption capacity of BCMC550 was observed to increase with an increasing temperature.

Table 5. Adsorption isotherm model parameters for CV adsorption onto BCMC550.

Temperature ($^{\circ}\text{C}$)	30	40	50	60
Langmuir				
q_m ($\text{mg}\cdot\text{g}^{-1}$)	625.0	714.3	714.3	909.1
K_L ($\text{L}\cdot\text{g}^{-1}$)	0.123	0.187	0.636	0.239
R_L	0.039	0.026	0.008	0.021
R^2	0.997	0.994	0.997	0.998
Freundlich				
K_F ($\text{mg}\cdot\text{g}^{-1}$)($\text{L}\cdot\text{mg}^{-1}$) $^{1/n}$	276.4	376.8	384.2	724.4
n	15.55	7.800	7.525	6.821
R^2	0.942	0.921	0.919	0.986

Table 6 provides a comparison of CV adsorption capacities on different biosorbents with those reported in previous studies. It can be observed that BCMC550 exhibits a significantly higher adsorption capacity compared to other adsorbents, classifying it as one of the most effective adsorbents in this context. The high maximum adsorption capacity T ($q_{\text{max}} = 909.1 \text{ mg}\cdot\text{g}^{-1}$) can be attributed to the cationic nature of CV, which readily adsorbs onto the functional groups present on the biochar surface. Furthermore, morphological studies revealed that BCMC550, obtained through thermal flash pyrolysis, is a well-developed porous material that allows CV dye to diffuse into the internal pore network of the biochar and become immobilized. The enhanced adsorption efficiency observed in this system is attributed to the pyrolysis process, which produces a rougher oxygen-rich surface with varied pore sizes, favoring the adsorption of CV dye.

Table 6. Comparison of the CV adsorption capacities of different biosorbents.

Adsorbent	q_{\max} (mg·g ⁻¹)	Reference
Activated carbon MO _{CA} -H ₃ PO ₄	469.55	[27]
Black Plum seed biochar (BPSB)	42.39	[34]
Fe ₃ O ₄ -coated biochar	349.4	[35]
Biochar (CB-LDH)	374.686	[36]
Woody tree biochar	125.5	[37]
Biochar derived from palm stalk	209	[38]
Fe ₃ O ₄ -graphene-rice straw-derived biochar	436.68	[39]
Magnetic biochar derived from rice straw	111.48	[40]
BCMC550	909.1	This study

3. Materials and Methods

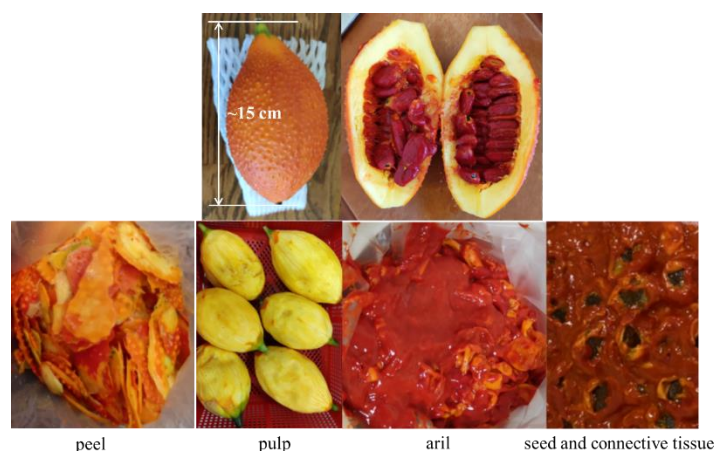
3.1. Materials

Gac fruit was sourced from local farms in Taitung County, Taiwan. Methanol ($\geq 99.5\%$) and ethanol ($\geq 99.8\%$) were obtained from Fisher Chemical, Hampton, NH, USA. Ascorbic acid ($\geq 99\%$), crystal violet (CV) and potassium persulfate ($\geq 99\%$) were supplied by Acros Organics, Geel, Belgium. DPPH (2,2-diphenyl-1-picrylhydrazyl) ($\geq 95\%$) was purchased from Alfa Aesar, Ward Hill, MA, USA, while ABTS (2,2'-azino-bis (3-ethylbenzothiazoline-6-sulphonic acid)) ($\geq 98\%$) was procured from Sigma-Aldrich, St. Louis, MO, USA. All chemicals were of HPLC grade and utilized without further purification.

3.2. Extraction Method

3.2.1. Pre-Treatment of Gac Fruit

Slice open the entire native gac fruit and segregate the pulp, peel, aril, and seeds, as shown in Figure 10. Subsequently, place the arils in a $-20\text{ }^{\circ}\text{C}$ refrigerator for a minimum of 3 days. Transfer the arils to a manifold freeze dryer set to a condensation temperature of $-60\text{ }^{\circ}\text{C}$ and vacuum pressure below 0.04 mbar for at least 7 days. Grind the dried arils into a powder using a mortar and sieve, aiming for a powder size of less than 20 mesh. Store the powdered arils in a sealed glass container and refrigerate at $4\text{ }^{\circ}\text{C}$ to complete the pretreatment. Following pretreatment, the proportions of pulp, peel, aril, and seed of the total weight of gac fruit were measured at 55.7%, 13.0%, 17.4%, and 13.8%, respectively. The proportion of the aril was 17.4%, which falls within the reported range of 6% to 31% [41]. These variations may be attributed to differences in variety, growing conditions, and the maturity of the fruits investigated [42]. The aril exhibited an average dehydration rate of approximately 75.2%, indicating a high water content as characteristic of gac fruit.

**Figure 10.** Anatomy of gac fruit.

3.2.2. Extraction of Active Components

The aril powder was introduced into the extraction solvent, and the beaker was sealed with a film before being placed in a constant temperature shaking water bath set to a shaking frequency of 100 rpm. Following extraction, the resulting extract was filtered using Whatman No. 6 filter paper via vacuum filtration, and subsequently purified using a vacuum concentration device with condensation set at 5 °C and a water bath at 40 °C. The extract yield was calculated as (weight of extract/weight of dried material) × 100%. Various operational factors can influence the efficiency of solvent extraction, including pre-treatment methods, solvent types, solid-to-liquid ratio (S/L ratio), and extraction temperature. This study investigates the influence of different variables on the extraction efficiency and assesses the antioxidant capacity of the extract through DPPH and ABTS free radical scavenging assays.

3.2.3. DPPH Free Radical Scavenging Assay

Following the method described by Shimada et al. [43] with some modifications, 50 mL of diluted extract was combined with 950 mL of 0.6 mM DPPH methanol solution and allowed to incubate at room temperature in darkness for 30 min. The absorbance at a wavelength of 515 nm was then measured using a UV/vis spectrophotometer (Thermo Scientific, Braunschweig, Germany). The scavenging rate was calculated using the formula $[1 - (\text{absorbance of sample at 515 nm} / \text{absorbance of blank at 515 nm})] \times 100\%$, and expressed as milligrams of ascorbic acid (AA) equivalents per gram of dry weight (mg AA equivalents·g⁻¹). A standard curve was constructed using various concentrations of ascorbic acid as the standard.

3.2.4. ABTS Free Radical Scavenging Assay

Adhering to the procedure outlined by Re et al. [44] with certain modifications, a 7.4 mM solution of ABTS and a 2.45 mM solution of potassium persulfate were prepared and combined in a 1:1 volume ratio and then left to incubate in darkness at room temperature for 12 h. Subsequently, the mixture was diluted with deionized water to achieve an absorbance of 1.0 ± 0.02 . Then, 50 mL of the diluted extract was mixed with 950 mL of the ABTS solution and allowed to stand in darkness at room temperature for 30 min. The absorbance of the resulting mixture was measured at a wavelength of 750 nm using a UV/vis spectrophotometer. The scavenging rate was calculated as $[1 - (\text{absorbance of sample at 750 nm} / \text{absorbance of blank at 750 nm})] \times 100\%$, and expressed as milligrams of ascorbic acid equivalents per gram of dry weight. Standard curves were constructed using various concentrations of ascorbic acid.

3.2.5. Extraction Kinetics Models

The data derived from the extraction experiments were utilized to ascertain the extraction rate constants. The solid–liquid extraction kinetics models employed encompassed first-order kinetic models and second-order kinetic models. The first-order kinetic model [45] is expressed as follows:

$$\frac{dC_t}{dt} = k_1(C_e - t) \quad (1)$$

After integrating and rearranging, we can obtain

$$\ln\left(\frac{C_e}{C_e - C_t}\right) = k_1 t + a \quad (2)$$

where k_1 is the overall mass transfer coefficient; a is a semi-empirical constant related to the loss of active ingredients, plant structure, and absorbed water; C_e is the equilibrium extraction yield (or ascorbic acid equivalent); and C_t is the extraction yield (or ascorbic acid equivalent) at any time (t), with k_1 and a as the parameters to be determined.

The second-order kinetic model [14] posits that under steady-state conditions, the extraction concentration remains uniform, and the concentration of the extracted product remains consistent under identical extraction conditions. The extraction yield (or ascorbic acid equivalent) can be represented by the following equation:

$$\frac{dC_t}{dt} = k_2(C_e - C_t)^2 \quad (3)$$

After integration of Equation (3) under the conditions of $C_t = 0$ at $t = 0$ and $C_t = C_t$ at $t = t$, Equation (4) can be obtained:

$$C_t = \frac{C_e^2 k_2 t}{1 + C_e k_2 t} \quad (4)$$

where k_2 is the second-order rate constant, and the parameters to be determined are k_2 and C_e .

3.3. Preparation of Adsorbent

The gac fruit peel was converted into biochar carbon using a slow pyrolysis method. The specific procedure involved drying the collected peel using freeze-drying, followed by storage in sealed bags with labels. A certain quantity of the dried peel was then placed in a quartz tube ($26 \times 30 \times 700$ mm) and pyrolyzed under a nitrogen gas atmosphere. The tube furnace parameters were set with a heating rate of $5 \text{ }^\circ\text{C}\cdot\text{min}^{-1}$, pyrolysis temperatures of 250, 350, 450, and 550 $^\circ\text{C}$, and a pyrolysis time of 1 h. After cooling to room temperature, the carbonized samples were removed and stored in a dryer for future use. The resulting biochars derived from gac fruit peel after post-carbonization were labeled as BCMC250, BCMC350, BCMC450, and BCMC550, corresponding to the respective pyrolysis temperatures. Scanning electron microscopy/Energy-dispersive X-ray spectrometry (SEM/EDS), elemental analysis (EA), specific surface area analysis using the Brunauer–Emmett–Teller (BET) method, and Fourier transform infrared spectroscopy (FTIR) are employed for the characterization of biochars.

3.4. Dye Adsorption Experiment

In this investigation, CV dye served as the model pollutant. The adsorbent, at a dosage of $0.5 \text{ g}\cdot\text{L}^{-1}$, was immersed in a dye solution with an initial concentration of 200 ppm, and the adsorption process was conducted at a temperature of 30 $^\circ\text{C}$. The system was then subjected to a constant temperature shaking water bath, and the adsorption kinetics of CV were monitored at intervals ranging from 0 to 480 min. The absorbance of CV dye on biochars was quantified using a UV/vis spectrophotometer at a peak wavelength of 590 nm, consistent with the approach of Sohni et al. [46]. The removal efficiency and adsorption capacity of the dye were computed according to the methodology outlined by Ma et al. [47]. The adsorption kinetic behavior of CV on the adsorbent was characterized using various adsorption kinetic models. Furthermore, the adsorbent, also at a dosage of $0.5 \text{ g}\cdot\text{L}^{-1}$, was exposed to varying concentrations of CV solutions, ranging from 200 to 600 ppm. These mixtures were similarly placed in a constant temperature shaking water bath, with the adsorption temperature set between 30 and 60 $^\circ\text{C}$. The optimization of adsorbent dosage and adsorption temperature conditions aligns with the work of Kosale et al. [34]. The adsorption process was allowed to proceed for 180 min, after which the adsorption isotherm data of CV were collected and analyzed using adsorption isotherm models. All the experiments were repeated independently at least three times.

4. Conclusions

This study investigates the extraction of Taiwan's native species of gac fruit, with a gac oil yield exceeding 50% and the highest antioxidant ability observed under the extraction conditions of 70 $^\circ\text{C}$, a solid-to-liquid (S/L) ratio of 1/9, and an extraction time of 120 min. The peel of the gac fruit, an underutilized agricultural waste, was

utilized to prepare biochar. This approach not only offers an eco-friendly solution to waste management but also explores a novel source material for biochar production and dye adsorption, which has not been extensively studied. The preparation of biochar from gac fruit peel involves environmentally benign processes, aligning with sustainable practices. The application of the waste for biochar production in dye removal studies indicates that BCMC550 biochar demonstrates the highest CV dye removal efficiency, attributed to its largest specific surface area ($697 \text{ m}^2 \cdot \text{g}^{-1}$), highest total pore volume ($0.31 \text{ cm}^3 \cdot \text{g}^{-1}$), and highest carbon content (62.98%). Our results demonstrated a significant adsorption capacity for CV dye, highlighting the efficacy of gac fruit peel biochar as an adsorbent. This suggests that BCMC550 may be effectively utilized to remove substantial amounts of cationic dyes from wastewater, in contrast to other adsorbents. This underscores the potential of converting waste materials into valuable adsorbents.

Author Contributions: Conceptualization and methodology, C.-T.C. and G.-B.H.; Investigation and formal analysis, N.-T.N., P.-R.C., R.-H.Y. and K.-J.C.; resources, C.-T.C. and G.-B.H.; data curation, P.-R.C.; Writing—original draft preparation, C.-T.C., N.-T.N. and G.-B.H.; writing—G.-B.H. All authors have read and agreed to the published version of the manuscript.

Funding: This research was funded by the Ministry of Science and Technology, Republic of China (Grant number: MOST 110-2221-E-027-127).

Institutional Review Board Statement: Not applicable.

Informed Consent Statement: Not applicable.

Data Availability Statement: Data are contained within the article.

Acknowledgments: The authors thank the Ministry of Science and Technology, ROC, Taiwan, for supporting this research financially. The authors thank the anonymous reviewers for their comments.

Conflicts of Interest: The authors declare no conflicts of interest. The funders had no role in the design of the study; in the collection, analyses, or interpretation of data; in the writing of the manuscript; or in the decision to publish the results.

References

1. Vuong, L.T. Underutilized β -carotene-rich crops of Vietnam. *Food Nutr. Bull.* **2000**, *21*, 173–181. [[CrossRef](#)]
2. Chuyen, H.V.; Nguyen, M.H.; Roach, P.D.; Golding, J.B.; Parks, S.E. Gac fruit (*Momordica cochinchinensis* Spreng.): A rich source of bioactive compounds and its potential health benefits. *Int. J. Food Sci. Technol.* **2015**, *50*, 567–577. [[CrossRef](#)]
3. Wong, R.C.; Fong, W.; Ng, T. Multiple trypsin inhibitors from *Momordica cochinchinensis* seeds, the Chinese drug mubiezhi. *Peptides* **2004**, *25*, 163–169. [[CrossRef](#)]
4. Chen, D.; Huang, C.; Chen, Z. A review for the pharmacological effect of lycopene in central nervous system disorders. *Biomed. Pharmacother.* **2019**, *111*, 791–801. [[CrossRef](#)]
5. Aoki, H.; Kieu, N.T.M.; Kuze, N.; Tomisaka, K.; Chuyen, N.V. Carotenoid pigments in GAC fruit (*Momordica cochinchinensis* Spreng.). *Bisoci. Biotechnol. Biochem.* **2002**, *66*, 2479–2482. [[CrossRef](#)]
6. Wong, Y.S.; Ariffin, F.D.; Ghazali, H.M. Effect of different drying techniques on the phytochemicals content and antioxidant activity of Gac fruit. *J. Food Sci. Technol.* **2019**, *56*, 2987–2994.
7. Kubola, J.; Siriamornpun, S. Phytochemicals and antioxidant activity of different fruit fractions (peel, pulp, aril, and seed) of Thai Gac (*Momordica cochinchinensis* Spreng.). *Food Chem.* **2011**, *127*, 1138–1145. [[CrossRef](#)]
8. Sroy, P.; Choe, S.; Heo, H.J.; Lee, J.H.; Jeong, S.M. Supercritical fluid extraction of carotenoids and tocopherols from Gac fruit. *J. Supercrit. Fluids* **2014**, *93*, 48–54.
9. Ahmad, M.; Rajapaksha, A.U.; Lim, J.E.; Zhang, M.; Bolan, N.; Mohan, D.; Vithanage, M.; Lee, S.S.; Ok, Y.S. Biochar as a sorbent for contaminant management in soil and water: A review. *Chemosphere* **2014**, *99*, 19–33. [[CrossRef](#)]
10. Tran, H.N.; You, S.J.; Chao, H.P.; Nguyen, V.N. Insight into adsorption mechanism of cationic dye onto agricultural residues-derived hydrochar: Negligible role of π - π interaction. *Environ. Sci. Pollut. Res. Int.* **2017**, *24*, 23217–23230. [[CrossRef](#)]
11. Adegoke, K.A.; Bello, O.S. Dye sequestration using agricultural wastes as adsorbents. *Water Resour. Ind.* **2015**, *12*, 8–24. [[CrossRef](#)]
12. Aksu, Z. Application of biosorption for the removal of organic pollutants: A review. *Process Biochem.* **2005**, *40*, 997–1026. [[CrossRef](#)]
13. Mittal, A.; Mittal, J.; Malviya, A.; Kaur, D.; Gupta, V.K. Adsorption of hazardous dye crystal violet from wastewater by waste materials. *J. Colloid Interface Sci.* **2010**, *343*, 463–473. [[CrossRef](#)]
14. Qu, W.; Pan, Z.; Ma, H. Extraction modeling and activities of antioxidants from pomegranate marc. *J. Food Eng.* **2010**, *99*, 16–23. [[CrossRef](#)]

15. Radha krishnan, K.; Sivarajan, M.; Babuskin, S.; Archana, G.; Axhagu Saravana Babu, P.; Sukumar, M. Kinetic modeling of spice extraction from *S. aromaticum* and *C. cassia*. *J. Food Eng.* **2013**, *117*, 326–332. [[CrossRef](#)]
16. Ponomaryov, V.D. *Medicinal Herbs Extraction*; Medicina: Moscow, Russia, 1976.
17. Peleg, M. An empirical model for the description of moisture sorption curves. *J. Food Sci.* **1988**, *53*, 1216–1219. [[CrossRef](#)]
18. Cacace, J.E.; Mazza, G. Optimization of extraction of anthocyanins from black currants with aqueous ethanol. *J. Food Sci.* **2003**, *68*, 240–248. [[CrossRef](#)]
19. Topallar, H.; Gecgel, U. Kinetics and thermodynamics of oil extraction from sunflower seeds in the presence of aqueous acidic hexane solutions. *Turk. J. Chem.* **2000**, *24*, 247–253.
20. Saxena, D.K.; Sharma, S.K.; Sambhi, S.S. Kinetics and thermodynamics of cottonseed oil extraction. *Grasas Aceites* **2011**, *62*, 198–205. [[CrossRef](#)]
21. Sant’Anna, V.; Brandelli, A.; Marczak, L.D.F.; Tessaro, I.C. Kinetic modeling of total polyphenol extraction from grape marc and characterization of the extracts. *Sep. Purif. Technol.* **2012**, *100*, 82–87. [[CrossRef](#)]
22. Lan, C.H.; Hanh, P.T.; Francisco, J.O.P.; Yves, W. Stability of carotenoid extracts of gac (*Momordica cochinchinensis*) towards cooxidation-Protective effect of lycopene on β -carotene. *Food Res. Int.* **2011**, *44*, 2252–2257.
23. Pradal, D.; Vauchel, P.; Decossin, S.; Dhulster, P.; Dimitrov, K. Kinetics of ultrasound-assisted extraction of antioxidant polyphenols from food by-products: Extraction and energy consumption optimization. *Ultrason. Sonochem.* **2016**, *32*, 137–146. [[CrossRef](#)] [[PubMed](#)]
24. Xu, Y.; Zhang, L.; Bailina, Y.; Ge, Z.; Ding, T.; Ye, X.; Liu, D. Effects of ultrasound and/or heating on the extraction of pectin from grapefruit peel. *J. Food Eng.* **2014**, *126*, 72–81. [[CrossRef](#)]
25. Shaaban, A.; Se, S.M.; Dimin, M.F.; Juoi, J.M.; Husin, M.H.M.; Mitan, N.M.M. Influence of heating temperature and holding time on biochars derived from rubber wood sawdust via slow pyrolysis. *J. Anal. Appl. Pyrolysis* **2014**, *107*, 31–39. [[CrossRef](#)]
26. Das, T.; Debnath, A.; Manna, M.S. Adsorption of malachite green by Aegle marmelos-derived activated biochar: Novelty assessment through phytotoxicity tests and economic analysis. *J. Indian Chem. Soc.* **2024**, *101*, 101219. [[CrossRef](#)]
27. Raji, Y.; Nadi, A.; Mechnou, I.; Saadouni, M.; Cherkaoui, O.; Zyade, S. High adsorption capacities of crystal violet dye by low-cost activated carbon prepared from Moroccan Moringa oleifera wastes: Characterization, adsorption and mechanism study. *Diam. Relat. Mater.* **2023**, *135*, 109834. [[CrossRef](#)]
28. Lamberti, E.; Viscusi, G.; Kiani, A.; Boumeough, Y.; Acocella, M.R.; Gorrasi, G. Efficiency of dye adsorption of modified biochar: A comparison between chemical modification and ball milling assisted treatment. *Biomass Bioenerg.* **2024**, *185*, 107247. [[CrossRef](#)]
29. Sing, K.S.W.; Everett, D.H.; Haul, R.A.W.; Moscou, L.; Pierotti, R.A.; Rouqu  rol, J.; Siemieniewska, T. Reporting physisorption data for gas/solid systems with special reference to the determination of surface area and porosity (Recommendations 1984). *Pure Appl. Chem.* **1985**, *57*, 603–619. [[CrossRef](#)]
30. Lagergren, S. Zur theorie der sogenannten adsorption geloster stoffe, Kungliga Svenska Vetenskapsademiens. *Handlingar* **1898**, *24*, 1–39.
31. Ho, Y.S.; McKay, G. Pseudo-second order model for sorption processes. *Process Biochem.* **1999**, *34*, 451–465. [[CrossRef](#)]
32. Langmuir, I. The constitution and fundamental properties of solids and liquids. *J. Am. Chem. Soc.* **1916**, *38*, 2221–2295. [[CrossRef](#)]
33. Freundlich, H.M.F. Uber die adsorption in lasungen. *Z. Phys. Chem.* **1906**, *57A*, 385–470.
34. Kosale, D.; Singh, V.K.; Thakur, C. Comparative adsorption of cationic and anionic dye by using non-activated Black Plum seed biochar for aquatic phase: Isotherm, kinetic and thermodynamic studies. *Ind. Crop. Prod.* **2024**, *215*, 118609. [[CrossRef](#)]
35. Sun, P.; Hui, C.; Khan, R.A.; Du, J.; Zhang, Q.; Zhao, Y.H. Efficient removal of crystal violet using Fe₃O₄-coated biochar: The role of the Fe₃O₄ nanoparticles and modeling study their adsorption behavior. *Sci. Rep.* **2015**, *5*, 12638. [[CrossRef](#)]
36. Tan, X.; Liu, Y.; Gu, Y.; Liu, S.; Zeng, G.; Cai, X.; Hu, X.; Wang, H.; Liu, S.; Jiang, L. Biochar pyrolyzed from MgAl-layered double hydroxides pre-coated ramie biomass (*Boehmeria nivea* (L.) Gaud.): Characterization and application for crystal violet removal. *J. Environ. Manag.* **2016**, *184*, 85–93. [[CrossRef](#)]
37. Wathukarage, A.; Herath, I.; Iqbal, M.C.M.; Vithanage, M. Mechanistic understanding of crystal violet dye sorption by woody biochar: Implications for wastewater treatment. *Environ. Geochem. Health* **2019**, *41*, 1647–1661. [[CrossRef](#)]
38. Chahinez, H.O.; Abdelkader, O.; Leila, Y.; Tran, H.N. One-stage preparation of palm petiole-derived biochar: Characterization and application for adsorption of crystal violet dye in water. *Environ. Technol. Innov.* **2020**, *19*, 100872. [[CrossRef](#)]
39. Du, C.; Song, Y.; Shi, S.; Jiang, B.; Yang, J.; Xiao, S. Preparation and characterization of a novel Fe₃O₄-graphene-biochar composite for crystal violet adsorption. *Sci. Total Environ.* **2020**, *711*, 134662. [[CrossRef](#)] [[PubMed](#)]
40. Yi, Y.; Tu, G.; Ying, G.; Fang, Z.; Tsang, E.P. Magnetic biochar derived from rice straw and stainless steel pickling waste liquor for highly efficient adsorption of crystal violet. *Bioresour. Technol.* **2021**, *341*, 125743. [[CrossRef](#)] [[PubMed](#)]
41. Parks, S.E.; Murray, C.T.; Gale, D.L.; Al-Khawaldeh, B.; Spohr, L.J. Propagation and production of Gac (*Momordica cochinchinensis* Spreng.), a greenhouse case study. *Exp. Agric.* **2013**, *49*, 234–243. [[CrossRef](#)]
42. Nhung, D.T.T.; Bung, P.N.; Ha, N.T.; Phong, T.K. Changes in lycopene and beta carotene contents in aril and oil of gac fruit during storage. *Food Chem.* **2010**, *121*, 326–331. [[CrossRef](#)]
43. Shimada, K.; Fujikawa, K.; Yahara, K.; Nakamura, T. Antioxidative properties of Xanthan on the autoxidation of soybean oil in cyclodextrin emulsion. *J. Agric. Food Chem.* **1992**, *40*, 945–948. [[CrossRef](#)]
44. Re, R.; Pellegrini, N.; Proteggente, A.; Pannala, A.; Yang, M.; Rice-Evans, C. Antioxidant activity applying an improved ABTS radical cation decolorization assay. *Free Radic. Biol. Med.* **1999**, *26*, 1231–1237. [[CrossRef](#)]

45. Jaganyi, D.; Wheeler, P.J. Rooibos tea: Equilibrium and extraction kinetics of aspalathin. *Food Chem.* **2003**, *83*, 121–126. [[CrossRef](#)]
46. Sohni, S.; Gul, K.; Shah, J.A.; Iqbal, A.; Sayed, M.; Khan, S.B. Immobilization performance of graphene oxide-based engineered biochar derived from peanut shell towards cationic and anionic dyes. *Ind. Crop. Prod.* **2023**, *206*, 117656. [[CrossRef](#)]
47. Ma, C.M.; Hong, G.B.; Wang, Y.K. Performance evaluation and optimization of dyes removal using rice bran-based magnetic composite adsorbent. *Materials* **2020**, *13*, 2764. [[CrossRef](#)]

Disclaimer/Publisher's Note: The statements, opinions and data contained in all publications are solely those of the individual author(s) and contributor(s) and not of MDPI and/or the editor(s). MDPI and/or the editor(s) disclaim responsibility for any injury to people or property resulting from any ideas, methods, instructions or products referred to in the content.